Carbohydrate Polymers 84 (2011) 1039–1047

Contents lists available at ScienceDirect

Carbohydrate Polymers

journal homepage: www.elsevier.com/locate/carbpol

Free radical graft copolymerization of nanofibrillated cellulose with acrylic monomers

Kuisma Littunen[a], Ulla Hippi[a], Leena-Sisko Johansson[b], Monika Österberg[b], Tekla Tammelin[c], Janne Laine[b], Jukka Seppälä[a,*]

[a] Polymer Technology, Department of Biotechnology and Chemical Technology, Aalto University School of Science and Technology, P.O. Box 16100, 00076 Aalto, Finland
[b] Forest Products Surface Chemistry, Department of Forest Products Technology, Aalto University School of Science and Technology, P.O. Box 16400, 00076 Aalto, Finland
[c] VTT Technical Research Centre of Finland, P.O. Box 1000, 02044 VTT, Finland

ARTICLE INFO

Article history:
Received 7 October 2010
Received in revised form
16 December 2010
Accepted 21 December 2010
Available online 25 December 2010

Keywords:
Nanofibrillated cellulose
Copolymerization
Grafting from
Acrylates
Methacrylates

ABSTRACT

Nanofibrillated cellulose (NFC) was graft copolymerized in aqueous suspension by a redox-initiated free radical method. Cerium ammonium nitrate was used as initiator. Acrylic monomers used in the grafting were glycidyl methacrylate, ethyl acrylate, methyl methacrylate, butyl acrylate, and 2-hydroxyethyl methacrylate. Effects of monomer type and concentration, initiator concentration and polymerization time on grafting from NFC were studied. Grafting was verified by several chemical characterizations and the synthesis method was found to be both efficient and selective for grafting. Overall, graft yields were higher than those reported in studies with macroscopic cellulose but surprisingly independent of the water solubility of each monomer. All modifications made NFC more hydrophobic, and some also improved its heat resistance. The structures formed by the grafted polymer varied from a thin coating to a matrix completely surrounding the nanofibrils. By performing the grafting in aqueous suspension, the nanofibrillar structure was retained.

1. Introduction

Nanofibrillated cellulose (NFC), which is prepared from wood pulp usually by a combination of mechanical and chemical or enzymatic treatments, is a promising material with many unique properties (Turbak, Snyder, & Sandberg, 1983). The fibrils are below 100 nm in diameter and may be micrometers long. Small diameter and large aspect ratio give the nanofibrils a large specific surface area, making NFC interesting as a filter material or reinforcement in polymer composites. The main challenges in using NFC are associated with the high polarity of cellulose. In addition, the numerous hydroxyl groups cause strong hydrogen bonds to form between cellulose chains and to bind water. In dilute water suspensions, the hydroxyl groups facilitate dispersion of the fibrils, but in non-polar solvent they promote formation of bundles and aggregates, with loss of the benefits of nano-scale dimensions. To avoid aggregation, NFC must be stored as a water suspension with less than 2 wt% solids content, which severely limits its large-scale industrial utilization (Berglund, 2005).

Chemical modification of NFC offers a way around these obstacles. A suitable polymer coating could both prevent aggregation and add reactivity towards other chemicals. Functionalized grafted polymer could also be exploited in further reactions such as cross-linking or used as reactive filter material. Cellulose can be grafted with polymers by attaching previously formed polymer chains to the cellulose backbone (*grafting onto*), by growing new polymer chains from radical sites on the backbone (*grafting from*), or by introducing vinylic groups to cellulose and copolymerizing the resulting macromonomer with a small molecular weight comonomer (*grafting through*) (Odian, 2004). Methods for grafting from cellulose have been extensively studied since 1960s, including radical polymerization of vinylic monomers (Geacintov, Stannett, Abrahamson, & Hermans, 1959; Roy, Semsarilar, Guthrie, & Perrier, 2009; Zahran & Mahmoud, 2003) and ring-opening polymerization of cyclic monomers (Habibi et al., 2008). Several auxiliary procedures to promote copolymerization have also been tested, among them thiocarbonation pre-treatment of cellulose to increase its reactivity towards radicals (Zahran & Mahmoud, 2003; Zahran, 2006) and adding alcohols or surfactants to the reaction mixture to improve the solubility of vinylic monomers (Gupta, Sahoo, & Khandekar, 2002; Okieimen, Uroghide, & Oriakhi, 1990). However, most studies have been done with macroscopic cellulose fibers and only a few with NFC (Stenstad, Andresen, Tanem, & Stenius, 2008).

The aim of this work was to modify NFC by graft copolymerization to make it more hydrophobic and to add new functionality, for example epoxide groups. Previous NFC grafting studies have dealt

* Corresponding author. Tel.: +358 9 4702 2614; fax: +358 9 462 373.
E-mail address: jukka.seppala@aalto.fi (J. Seppälä).

0144-8617/$ – see front matter © 2011 Elsevier Ltd. All rights reserved.
doi:10.1016/j.carbpol.2010.12.064

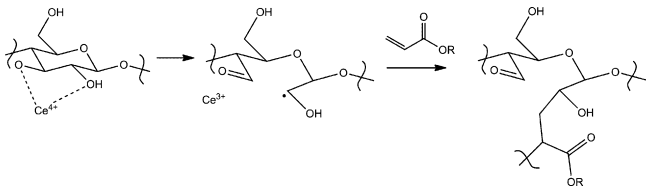

Scheme 1. Mechanism of cerium initiated copolymerization (Mishra et al., 2003).

with single monomers only. Instead, we wanted to carry out an extensive comparison of different monomers, for which acrylates and methacrylates are suitable, since they are available as many different derivatives and are readily polymerized by radical methods. A free radical copolymerization initiated by ammonium cerium(IV) nitrate ($(NH_4)_2Ce(NO_3)_6$, CAN) was selected for the experiments, as it has been thoroughly tested and is a selective method for grafting of polysaccharides (O'Connell, Birkinshaw, & O'Dwyer, 2005; Okieimen, 2003). Most importantly, the whole synthesis can be carried out in an aqueous medium, without the tedious solvent exchange required by many controlled copolymerization methods (Jenkins & Hudson, 2001). The initiation occurs via a redox reaction as the cerium ion chelates with two adjacent hydroxyl groups in a cellulose chain, resulting in radical formation on an opened glucose ring. This mechanism is illustrated in Scheme 1 (Mishra, Srinivasan, & Gupta, 2003). Several acrylates and methacrylates were used as monomers, and differences in their reactivity were determined. Chemical and physical properties of the products were thoroughly characterized.

2. Experimental

2.1. Materials

NFC was prepared at VTT Technical Research Centre of Finland by mechanical disintegration (Paakko et al., 2007). Bleached birch pulp was pre-treated with a Voith refiner and then fluidized by seven passes through an M7115 fluidizer from Microfluidics Corp (Newton, MA, USA). The solids content of the prepared water dispersion was 1.6 wt%, with a xylan content of 25%. Glycidyl methacrylate (GMA), ethyl acrylate (EA), and 2-hydroxyethyl methacrylate (HEMA) were obtained from Sigma–Aldrich (St. Louis, MO, USA), methyl methacrylate (MMA) was from Merck (Whitehouse Station, NJ, USA), and butyl acrylate (BuA) was from Sigma–Aldrich (St. Louis, MO, USA). All monomers were filtered through aluminum oxide to remove inhibitor (hydroquinone monomethyl ether) and stored in a freezer. Nitric acid and ammonium cerium (IV) nitrate (CAN) were purchased from Sigma–Aldrich and used as received. Acetone and THF were procured from VWR (Karlskoga, Sweden) and methyl ethyl ketone (MEK) and toluene from Merck. Methanol was from Sigma–Aldrich, diethyl ether (DEE) from Riedel-de Haën (Seelze, Germany), and isooctane from Rathburn Chemicals (Walkerburn, UK). All solvents were analytical reagent grade.

2.2. Graft copolymerization

NFC/water suspension was diluted to 0.2 wt% and adjusted to pH 1 with diluted nitric acid. Nitrogen was bubbled through the mixture, CAN was added as an initiator after 15 min of stirring, and the mixture was stirred for another 15 min while heated to 35 °C. Monomer was added gradually over a period of 30 min, and the mixture was stirred for a further 30 or 60 min. The initiator concentration was 2 or 4 mmol/dm^3 and the amount of monomer was 20 or 40 mmol per g of dry NFC.

The reaction mixture was centrifuged, and the solid substance was washed with water to remove the traces of initiator and acid. The solid was then washed with acetone and THF to separate the homopolymer from the graft copolymer, except NFC-g-PHEMA, which was washed with methanol instead. The washing solutions were poured into an appropriate nonsolvent (Bloch, 1999) and the precipitated homopolymer was centrifuged. Methanol was used as a nonsolvent with PGMA, PMMA, and PBuA. Isooctane was used with PEA and DEE with PHEMA. The grafted NFC and homopolymer were dried overnight at room temperature.

2.3. Isolation of grafted polymer

Cellulose backbone was hydrolyzed by a method adapted from Shen and Huang (2004). 100–200 mg of grafted NFC was mixed in a flask with 10 ml of acetone and 15 ml of THF. After addition of 1 ml of concentrated sulfuric acid (72 wt%), the mixture was refluxed at its boiling point overnight. Resulting brown slurry was poured into a nonsolvent, and the precipitated polymer was washed with the same nonsolvent, dissolved, filtered, and precipitated again. Cleaved and purified polymer was dried at room temperature.

2.4. Characterization

2.4.1. Gravimetric calculations

Grafted NFC and retrieved homopolymer were weighed, and the results were used to calculate monomer conversion, graft yield, graft efficiency, and polymer weight fraction in each product with formulas (1)–(4):

$$\text{Conversion} = C = \frac{m_G + m_P}{m_M} \times 100\% \quad (1)$$

$$\text{Graft yield} = G = \frac{m_G}{m_{Cell}} \times 100\% \quad (2)$$

$$\text{Graft efficiency} = G_E = \frac{m_G}{m_G + m_P} \times 100\% \quad (3)$$

$$\text{Polymer weight fraction} = w_G = \frac{m_G}{m_G + m_{Cell}} \times 100\% \quad (4)$$

where m_G is the mass of the grafted polymer; m_P is the mass of the homopolymer; m_M is the mass of the fed monomer; m_{Cell} is the mass of the cellulose.

2.4.2. Determination of molar masses

Molar masses of homopolymers and successfully cleaved grafted polymers were determined on gel permeation chromatography (GPC) equipment including a Waters 510 HPLC pump, PLgel columns with 10 μm bead size, a Waters 2414 refractive index (RI) detector, and a Wyatt DAWN 8+ Heleos MALLS detector. Chloroform was used as an eluent, and the calibration curve was obtained with polystyrene standards.

2.4.3. Chemical characterization

FTIR spectra of the starting material and all products were recorded on a Nicolet 750 Magna device as an attenuated total reflection (ATR) measurement to verify the presence of new functional groups after modification. Solid-state NMR studies were performed with powdered samples (one sample of each type of copolymer) on a 270 MHz Chem-Magnetics CMX Infinity NMR spectrometer. The XPS characterizations were done with a Kratos AXIS 165 electron spectrometer with monochromatic Al Ka radiation at 100 W and high resolution measurements in carbon C 1s and oxygen O 1s regions were used.

2.4.4. Topographic microstructure

One sample of NFC grafted with PGMA, PEA, PBuA, and PHEMA was studied by atomic force microscopy (AFM) imaging to determine whether the nanostructure of NFC had been preserved. AFM samples of NFC-g-PGMA and NFC-g-PHEMA were prepared from never-dried dispersions by spin-coating on both hydrophilic and hydrophobic SiO_2 surfaces. Products grafted with PEA and PBuA were redispersed because they separated completely from the liquid phase during synthesis. These samples were sonicated in toluene at 50 W power for 5 min before spin-coating.

The samples were imaged in air in tapping mode with a Nanoscope IIIa Multimode scanning probe microscope from Digital Instruments Inc. (Santa Barbara, CA, USA). Silicon cantilevers (NSC15/AIBS) from MicroMasch (Tallinn, Estonia) were used. The drive frequency of the cantilever was about 300–360 kHz. At least three different 5 μm × 5 μm areas per sample were scanned.

2.4.5. Material properties

The appearance and dispersability of modified NFC were investigated in various solvents during washing. Dried products were visually evaluated, and their hydrophobicity was examined qualitatively by observing a water droplet on the product's surface.

Thermal behavior of products was characterized by differential scanning calorimetry (DSC) and thermogravimetric analysis (TGA). DSC was performed with a Mettler Toledo Star DSC 821e equipment. Temperature ranges for each polymer were selected according to glass transition temperatures (T_g) found in the literature (Andrews & Grulke, 1999). Experimental T_g values were determined during the second heating period at 10 °C/min. TGA was performed with a Seiko Instruments TG/DTA320 instrument and the measurements were done with two samples of NFC grafted with each monomer. Samples were heated under argon atmosphere from 25 to 500 °C at 10 °C/min.

3. Results and discussion

NFC was grafted with two acrylates and three methacrylates, and the composition of the products was gravimetrically determined. The products were characterized by FTIR, ^{13}C NMR, and XPS spectroscopy, AFM imaging, DSC, and TGA.

3.1. Graft copolymerizations

Monomer conversion (C), graft yield (G), graft efficiency (G_E), weight fraction (w_G), weight average molar mass, and polydispersity of the grafted polymer are displayed in Table 1. Homopolymer molar mass data is included in Appendix A.

Some degree of grafting was achieved with all tested monomers. GMA and alkyl acrylates grafted readily, forming a two- to fourfold amounts of grafted polymer relative to the amount of NFC. MMA, too, formed a significant amount of grafted polymer. HEMA was the only monomer that produced clearly less than 100% graft yield. Compared with some previous studies (Gupta et al., 2002; Zahran, 2006) carried out with macroscopic cellulose, the graft yields with EA and MMA were about 50% higher, using the same reaction time and only 1/10 of the initiator concentration. In a similar comparison, the graft yield obtained with GMA was 6, and with BuA as much as 12 times as high as on cellulose fibers. This kind of improvement was expected owing to much larger reactive surface area. Surprisingly, though, there was no correlation between the water solubility of the monomer and its reactivity toward cellulose in water solution.

Graft efficiency was excellent for glycidyl methacrylate, which formed almost no homopolymer. Alkyl acrylates also formed grafted products with over 80% graft efficiency. MMA grafted reasonably well from the NFC surface, though with a lower conversion,

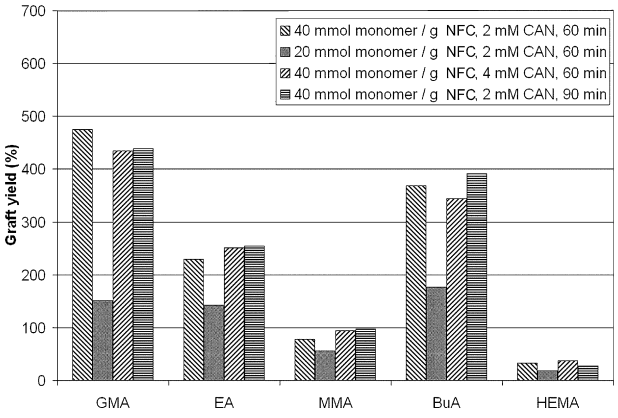

Fig. 1. The effects of monomer amount, initiator concentration, and polymerization time on the graft yield.

considerable amount of homopolymerization, and the weight fraction of polymer below 50%. HEMA was less prone to graft, but some polymerization occurred both from the NFC and as homopolymer. Conversion was as low as about 10% except with prolonged polymerization time. The dominant form of polymerization was then homopolymerization, seen as very low graft efficiency. The low graft efficiency probably arises from the initiator, which may form radicals on the carbon atom next to the hydroxyl group (Odian, 2004).

Study was made of the effects of initial monomer and initiator concentrations and polymerization time on the graft yield (Fig. 1).

The graft yield increased in a linear fashion with all monomer types except GMA as the initial monomer concentration was doubled. A somewhat steeper rise was observed with GMA. At the same time, the graft efficiency decreased slightly with EA and MMA, which is an indication of more homopolymer formation.

Initiator concentration of 2 mmol/dm^3 produced the same graft yield as a doubled amount did. And since a trial made with GMA and EA with even lower initiator concentration again resulted in a similar amount of grafting, we concluded that a very low amount of initiator was sufficient.

Increasing the polymerization time from 60 to 90 min caused a slight increase in the graft yield and graft efficiency. Thus, more graft polymerization than homopolymerization still occurred between 60 and 90 min, but an almost equal amount of grafted product was synthesized within 1 h.

Molar masses were successfully determined for all homopolymers except PHEMA, which was insoluble in available GPC solvents (chloroform and THF). Grafted polymer was successfully cleaved from NFC grafted with PEA, PMMA, and PBuA. The MALLS detector was used with PEA samples because the amount of soluble PEA in hydrolysis products was too low to show up in the RI detector. The Molar masses of grafted PGMA could not be determined because hydrolysis of the NFC-g-PGMA samples failed. The effects of monomer amount, initiator concentration, and polymerization time on molar mass are displayed in Fig. 2.

Molar mass of the grafted polymer varied widely with the monomer. Butyl acrylate clearly formed the longest grafts, the weight average molar masses being as much as 3500 kg/mol. Ethyl acrylate and methyl methacrylate were grafted in much shorter (but still relatively long) chains of about 100–400 kg/mol. Decrease in the amount of MMA and BuA also lowered the molar mass of the grafted polymer. Likewise for MMA and BuA, a higher initiator concentration had a distinct, although somewhat weaker effect on the molar mass. Both these results were in agreement with theoretical predictions. Longer polymerization time produced grafted polymer with clearly higher molar mass in the case of EA, but noticeably

Table 1
Polymerization parameters and gravimetrically determined conversion (C), graft yield (G), graft efficiency (G_E) and weight fraction of polymer (w_G) in each product.

Sample	n (M)/m(NFC)[a] (mmol/g)	[CAN] (mmol/dm^3)	t (min)	C[b] (%)	G[b] (%)	G_E[b] (%)	w_G[b] (%)	$M_{w,G}$ (kg/mol)	PD_G
NFC-PGMA 3	38	2	60	85	321	96	76	–	–
NFC-PGMA 4	20	2	60	54	146	96	59	–	–
NFC-PGMA 5	40	4	60	78	434	97	81	–	–
NFC-PGMA 6	40	2	90	77	439	99	81	–	–
NFC-PEA 4	20	2	60	82	95	–	49	33[d]	1.5
NFC-PEA 5	40	2	60	70	230	81	70	40[d]	4.9
NFC-PEA 6	40	4	60	74	251	84	72	391[d]	1.9
NFC-PEA 7	40	2	90	74	255	85	72	127[d]	2.6
NFC-PMMA 1	40	2	60	35	78	56	44	256[c]	2.0
NFC-PMMA 2	21	2	60	36	56	75	36	121[c]	1.5
NFC-PMMA 3	40	4	60	35	94	67	48	194[c]	1.7
NFC-PMMA 4	40	2	90	41	98	60	49	239[c]	1.9
NFC-PBuA 1	41	2	60	81	369	86	79	3480[c]	1.2
NFC-PBuA 2	20	2	60	81	177	85	64	1420[c]	1.8
NFC-PBuA 3	40	4	60	81	345	83	78	1890[c]	1.4
NFC-PBuA 4	40	2	90	86	392	89	80	1770[c]	1.7
NFC-PHEMA 1	40	2	60	10	33	63	25	–	–
NFC-PHEMA 2	21	2	60	14	19	51	16	–	–
NFC-PHEMA 3	40	4	60	11	37	64	27	–	–
NFC-PHEMA 4	40	2	90	29	27	18	21	–	–

[a] Quantity of monomer per gram of dry NFC.
[b] Determined gravimetrically.
[c] Determined by GPC.
[d] Determined by MALLS.

lower molar mass in the case of BuA (columns 1 and 4). The result for BuA was unexpected since, according to the theory of free radical polymerization, the number of radicals typically decreases faster than the number of monomer molecules, so that polymer chains that form later become longer (Odian, 2004). The reaction in question is a somewhat unusual free radical polymerization, however, because the radicals are not situated on small molecules or free polymer chains but on the surface of fibrils. Such macroradicals might terminate very slowly due to steric factors, explaining the discrepancies in the kinetics of the polymerization.

The molar mass of the grafted PMMA was fairly independent of all changes in the reaction parameters, except the amount of monomer. The lack of effect of the other parameters indicated a somewhat limited ability of MMA to graft copolymerize with cellulose and its higher tendency to homopolymerize. GPC analysis of grafted PEA gave inconsistent values, with a large, unexplained variance, possibly because the samples had a significant insoluble fraction that may skew the molar mass distribution.

Commercial PMMA (LG, Mn = 70 kg/mol) was subjected to a similar treatment to investigate the possible degrading effect of the sulfuric acid hydrolysis on the grafted polymer chains. No degradation of the molar mass was observed.

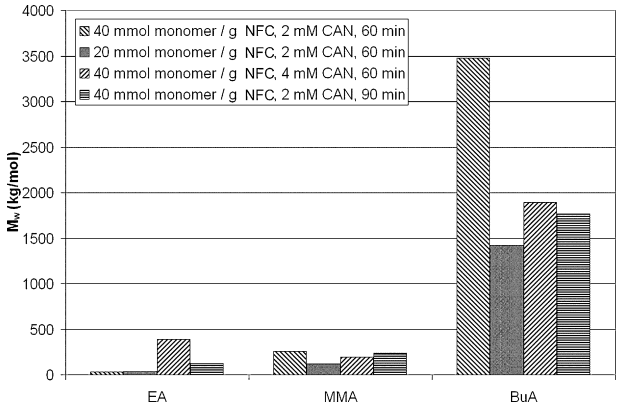

Fig. 2. The effects of monomer amount, initiator concentration, and polymerization time on the weight average molar mass of the grafted polymer.

3.2. Chemical characterization

Chemical structure of the unmodified NFC and the graft copolymers was characterized by FTIR, solid-state ^{13}C NMR and XPS. As an example, the FTIR spectra of unmodified NFC and NFC-g-PGMA, and an NMR spectrum of NFC are displayed in Fig. 3. Additional FTIR and NMR spectra are included in Appendix A.

The unmodified NFC shows a broad, strong absorption at about 3300 cm^{-1} resulting from abundant hydrogen bonded hydroxyl groups, and a somewhat weaker absorption at 2898 cm^{-1} due to C-H stretching. All the grafted NFC samples showed a new, strong absorption band at 1710–1730 cm^{-1}, characteristic of an ester carbonyl group. Characteristic C–H stretching peaks of the ester pendant groups were also observed in the area of 2960–2850 cm^{-1}. In addition, the samples grafted with PGMA had a medium strength absorption at 840 cm^{-1}, characteristic of an epoxy group (Hase, 1999).

NMR spectroscopy was tested as a means to quantify the chemical composition of the products. Solid-state NMR spectra were recorded from the unmodified NFC and one sample of NFC grafted with each monomer, and peak integrals were used to calculate the ratio of NFC to grafted polymer. In the spectrum of unmodified NFC (Fig. 3), signals of C_2 to C_6 were partially overlapping, but C_1 bonding to two oxygen atoms gave a well-defined signal at 107 ppm, which was used in the calculations. In the spectra of NFC grafted with polymers, peaks of carbon atoms of the grafted polymer were successfully assigned, even though there was some overlapping with cellulosic signals. In the case of NFC-g-PMMA, the peak at 18 ppm resulting from the methyl group in the polymer backbone was used in the calculations. The NFC/PMMA ratio calculated from the NMR spectrum (43 wt%) correlated well with the gravimetric value (44 wt%). The same peak at 16 ppm was used for NFC-g-PGMA, and the peak at 17 ppm for NFC-g-PHEMA. Again ratios were in accordance with the gravimetric results. Polyacrylates lack similar methyl groups but produced distinct peaks originating from the alkyl chains, at 15 ppm for PEA and 32 ppm for PBuA, which were used in calculating the ratios. There was a significant difference between the two characterization methods. For the samples of NFC grafted with PEA or PBuA, the NMR method gave too low a polymer content.

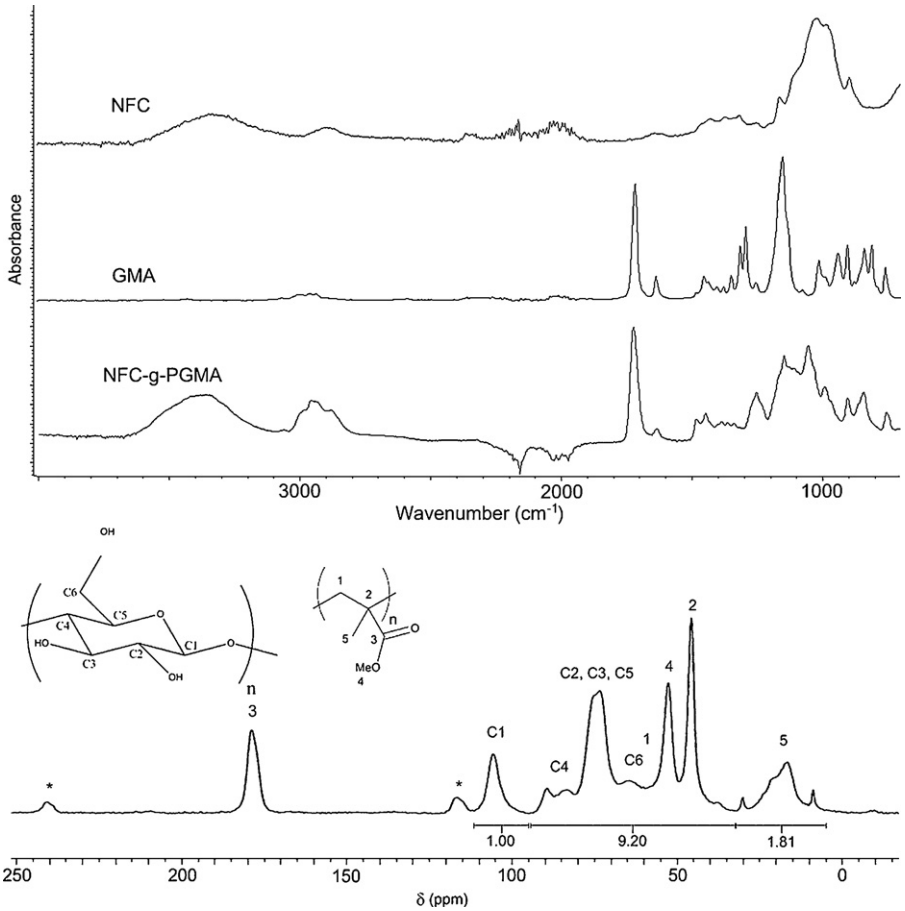

Fig. 3. FTIR spectra of neat NFC, GMA, and NFC-g-PGMA (above), and ^{13}C NMR spectrum (below) of NFC grafted with PMMA. Signals from cellulosic carbon atoms are labeled C1–C6 and signals from polymeric carbon atoms 1–5. Carbonyl side bands are marked with an asterisk (*).

XPS analysis was carried out on the unmodified NFC and samples grafted with GMA, MMA, and BuA. Low resolution survey spectra (Appendix A) showed only carbon and oxygen present at the surface. High resolution carbon C 1s spectra yielded information on the relative abundance of carbon atoms in different molecular environments (Fig. 4). The symmetric Gaussian four-component fit, that was used, is based on carbons with 0, 1, 2, or 3 bonds to oxygen. The component for carbon without oxygen neighbors (nonpolar carbon) is at the lowest binding energy, at 285.0 eV, and carboxylic carbons, having three bonds to oxygen, show up at the highest binding energy (Beamson & Briggs, 1992).

In the unmodified NFC (Fig. 4a), the main components in C 1s spectra were C–O and O–C–O bonds, characteristic of cellulose. In grafted samples, the modifications showed up as changes in distribution of the carbon component.

According to the XPS carbon data, the GMA grafted NFC, with 76 wt% of polymer, had practically no O–C–O-signal in the XPS spectrum (Fig. 4b). Furthermore, the ratios of C–C, C–O, and carboxyl components in the fitted C 1s data were close to 3:3:1, which is the stoichiometric ratio of PGMA. This indicates that a dense layer of grafted polymer had almost fully attenuated the signal for cellulose of the nanofibril backbone.

In the case of BuA and MMA grafted NFC's (Fig. 4c and c), the XPS carbon data had components from both the polymer and NFC, indicating only partial coverage of the fibrils. For the BuA grafted NFC, the surface content derived from XPS carbon compounds was similar to the bulk content (79 wt% vs. 80% of C (tot)). For the MMA-grafted NFC, the material with only 44 wt% polymer content, the surface was clearly enriched with the polymer, since over 60% of surface carbon species were identified as belonging to the polymer.

Note: According to XPS, the NFC reference surface contained more nonpolar carbon (carbon without oxygen neighbors) than would be expected for pure conventional celluloses. In conventional 100% cellulose specimens, this non-cellulosic carbon component is present but unusually low for an air-exposed surface (typically 2–5% of total carbon). This component has been explained as a combination of natural surface passivation layer and traces of non-cellulosic components present in the nature-derived material (Andresen, Johansson, Tanem, & Stenius, 2006). However, for NFC materials the amount of this non-cellulosic carbon tends to be much higher, although the material itself has been tested to be of very pure cellulose (Uschanov et al., 2010). The reason for this seems to lie in the properties of the NFC surface. Because of the marked increase in surface area of NFC as compared to the conventional celluloses, there is also a huge increase in the active OH-bonds at the surface. This property easily turns nanocelluloses into gels in aqueous conditions and these OH bonds strongly affect the surface passivation requirements, when fibrils are transferred into non-aqueous conditions (i.e., when water is replaced with air or with a non-polar solvent).

It should be noted that this chemical characterization data does not allow us to state conclusively that the polymers were grafted from cellulose because hemicellulose (xylan) was present in significant amounts in the starting material and is chemically very similar to cellulose. Nevertheless, the insolubility of the polymer shows that the polymer is firmly bonded to the nanofibrils.

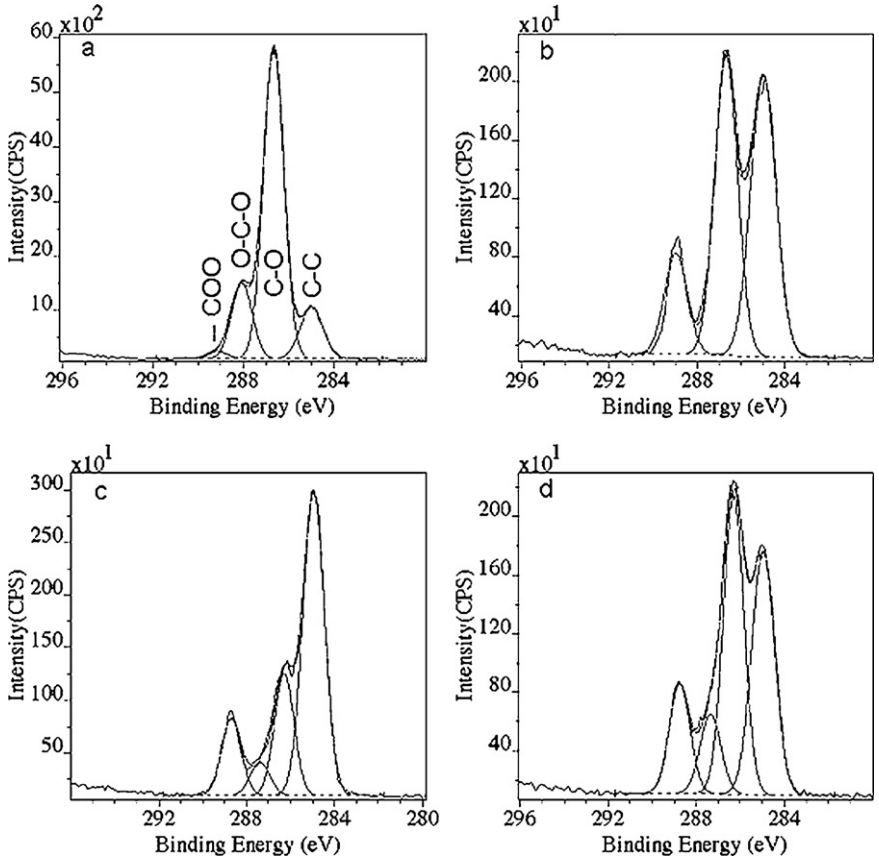

Fig. 4. High resolution carbon spectra of (a) non-modified NFC and NFC's grafted with (b) GMA, (c) BuA, and (d) MMA.

3.3. Topographic microstructure

Topographic AFM micrographs of unmodified NFC, NFC-g-PGMA (76%), and NFC-g-PHEMA (21%), as well as topographic and phase images of NFC-g-PEA and NFC-g-PBuA are presented in Fig. 5.

The unmodified NFC (Fig. 5a) consisted of fibrils that were clearly less than 50 nm in diameter, but thicker fibril aggregate bundles were also present. Comparison of the images reveals that the nanoscale fibrillar structure is retained during the graft copolymerization process. The grafted NFC samples showed a rougher surface than those of the unmodified NFC. The fibrils of the grafted NFC were also somewhat thicker than those of the unmodified sample, perhaps because of the large amount of grafted polymer. In NFC-g-PGMA, where the weight fraction of grafted PGMA was high (80%), the polymer was clearly visible as a granular structure on the nanofibrils (Fig. 5b), whereas in NFC-g-PHEMA, where the weight fraction was low (21%), the presence of polymer was seen as a rough surface of cellulose fibrils (Fig. 5c).

The polymer content was 70% in the NFC-g-PEA sample (M_w = 40 kg/mol, Fig. 5d–e) and 80% in the NFC-g-PBuA (1770 kg/mol, Fig. 5f–g). Although the polymer content of these samples was roughly equal to that of the NFC-g-PGMA sample, the topography was noticeably different. Instead of individual fibrils covered with a granular polymer phase, as seen in Fig. 5b, a more continuous polymer film was observed for both samples, and the fibrils were embedded in the polymer phase. In the case of the PEA-grafted sample, the fibrils were still visible in both the topography and phase images, but the PBuA grafts evidently reach so far out from the fibril surface that the polymer phase covered all the fibrils, and the existence of fibrils was evident only in the phase image.

Since the polymer appears to fully cover the fibrils, the phase shift is probably due to the difference in elasticity between fibrils and polymer. Another reason for the phase shift could be the difference in affinity between the measuring tip and the hydrophobic polymer chains or hydrophilic nanofibrils. In the NFC-g-PEA sample, the grafted polymer layer on the fibrils is so thin that the harder fibrils are clearly visible in the phase image. However, the grafted PBuA forms such a thick layer on the fibrils that they are hardly visible at all. The difference between these two samples could be explained by the much larger molar mass of PBuA grafts and the slightly higher polymer content in the samples. These observations were also supported by the GPC results, which were presented above.

The AFM and XPS results indicated slightly different behavior of the samples because of the different sample preparations. For AFM analysis the grafted NFC samples were spin-coated on hydrophilic silica, and the conformation of the polymer chain is affected according to its affinity to cellulose. As a consequence, fibrils were clearly visible in the AFM image of the NFC-g-PGMA sample, whereas full coverage of cellulose was indicated in the XPS analysis.

For NFC-g-PBuA, the AFM analysis indicated full coverage of the fibrils, whereas XPS indicated 80% coverage. These results are in good accordance, since the thickness of the film covering the fibrils observed in AFM can be well below the penetration depth of XPS, which for porous samples may be up to 10 nm.

Individual nanofibrils were seen in all modified samples, which indicates that the studied modification preserves the fine structure of NFC. Note that the PEA and PBuA grafted samples were prepared from dried material, and the differences between the two samples could be due to the much smaller molar mass of the PEA grafts. In the case of PEA, the polymer phase covering the fibrils

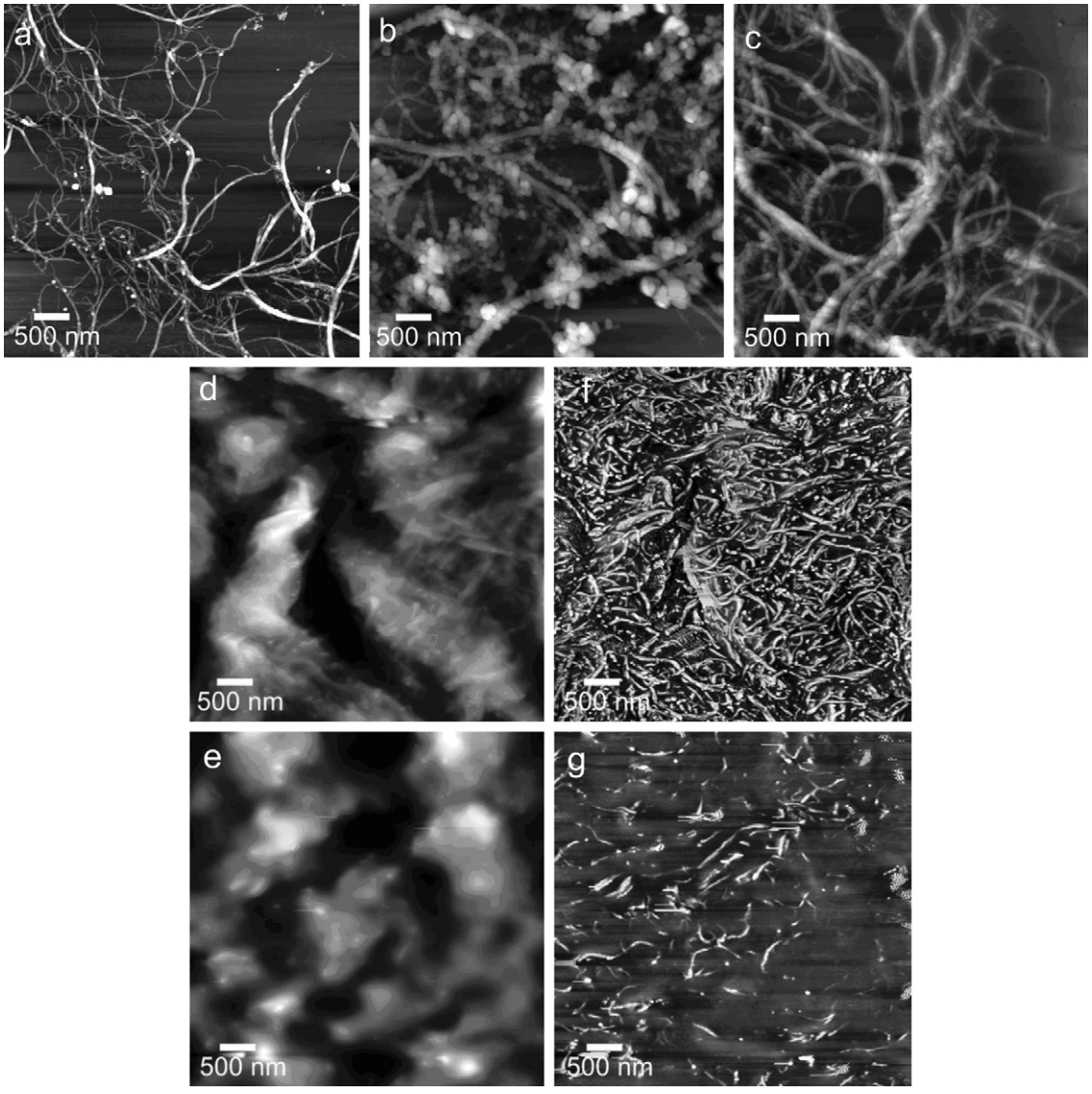

Fig. 5. AFM topographic images (5 μm × 5 μm) of (a) unmodified NFC, (b) NFC-g-PGMA, (c) NFC-g-PHEMA, (d) NFC-g-PEA, and (e) NFC-g-PBuA. Phase images of (f) NFC-g-PEA and (g) NFC-g-PBuA.

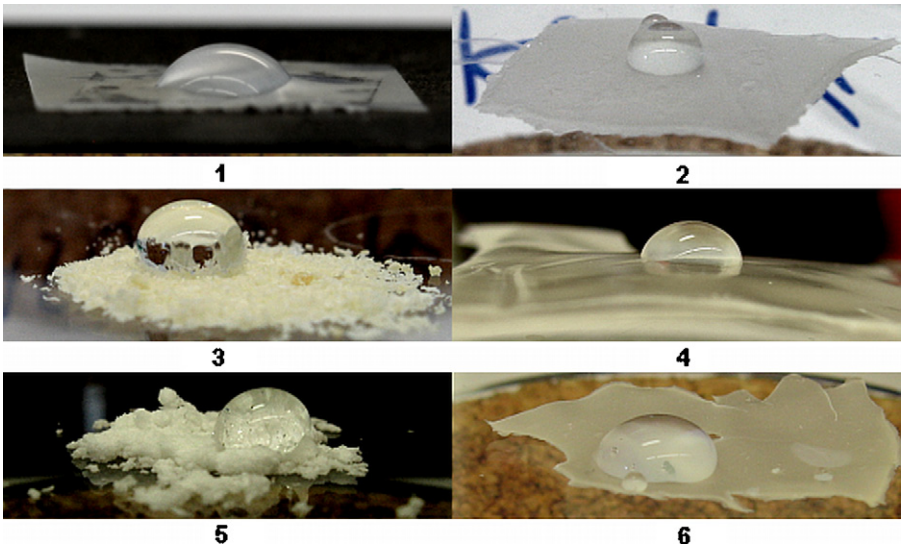

Fig. 6. Water droplet on the surface of unmodified NFC (1) and products grafted with PGMA (2), PEA (3), PMMA (4), PBuA (5), and PHEMA (6).

Table 2
Experimental glass transition temperatures of graft copolymers and separated homopolymers, literature reference values, and measured decomposition temperatures.

Polymer	T_g (grafted) (°C)	T_g (homopolymer) (°C)	T_g (literature)[a] (°C)	T_d [b] (°C)
NFC	–	–	–	246
PGMA	–[c]	66–70	63–74	177–198[e]
PEA	−16 to −14	−19 to −17	−24	250–254
PMMA	114[d]	103–116	105	256–267[e]
PBuA	−50 to −46	−49 to −47	−54	265–266
PHEMA	–[c]	80–90	85	–[f]

[a] Andrews and Grulke (1999).
[b] Initial decomposition temperature.
[c] T_g was vague or not observed.
[d] Only one successful measurement.
[e] Slow decay already at lower temperatures.
[f] Not analyzed due to the low polymer content.

is much thinner, and the grafted polymer may also be distributed more evenly on the fibrils. The polymer content was also slightly lower.

3.4. Material properties

Immediately after synthesis the NFC grafted with PGMA and PMMA was still dispersed in water as a milky mixture. The solid substance had nevertheless formed visible particles, which descended to the bottom relatively quickly. In acetone and THF, these products formed a stable dispersion, resembling unmodified NFC in water. Products containing PEA and PBuA were much more hydrophobic and precipitated from water as considerably larger particles. When the solvent was replaced by a less polar one, the particles were better dispersed. In the least polar solvent (toluene), the modified NFC seemed to swell and become translucent (Appendix A). Grafting with PHEMA did not change the appearance of water suspension, and the product was well dispersed both in water and methanol.

When dried, the well-dispersed products formed a fragmented film or a solid mass, whereas the granular products retained their form (Fig. 6).

Grafting with all tested monomers made NFC more hydrophobic. A clear effect was observed even with the fairly hydrophilic PHEMA modification. The samples grafted with PEA and PBuA were especially hydrophobic, although they were not entirely comparable to filmy products since the hydrophobicity of a surface is also affected by its roughness (Marmur, 2008). In addition, the difference between PMMA and PEA grafted NFC can be explained by the higher polymer content of the latter, rather than a difference in polarity (MMA and EA are isomers).

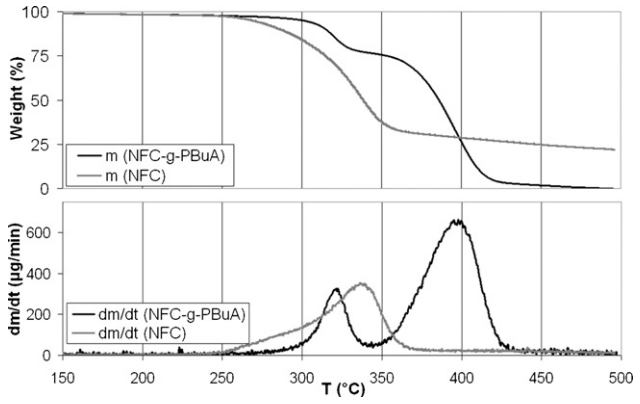

Fig. 7. Weight (above) and weight decreasing rate (below) of pure and PBuA grafted (80% PBuA) NFC as a function of temperature.

Glass transition temperatures (T_g) of the grafted products and homopolymers measured with DSC are presented in Table 2 along with T_g values of separated homopolymers, the reference values found in the literature (Andrews & Grulke, 1999), and the initial decomposition temperatures of the copolymers.

The observed temperatures were consistent with the T_g values of the homopolymers. Glass transition temperature could not be determined for grafted PGMA and PHEMA. Successfully measured values differed slightly from those reported in literature, probably because of the faster heating rate that we used, which generally gives less accurate results. Thermal decomposition behavior was not observed with this method although the samples were heated to 300 °C.

In TGA analysis, the unmodified NFC started to decompose close to 250 °C and exhibited a sharp drop in weight leading to an almost complete degradation below 400 °C. A significant increase in initial decomposition temperatures was observed for samples grafted with PEA and PBuA, about 10 and 20 °C, respectively. Measurements of NFC-PBuA and pure NFC are shown as an example in Fig. 7. With other modifications, there was only a negligible increase, or even a decrease, relative to the unmodified sample. The amount of grafted polymer had much less effect on the decomposition behavior than did the type of monomer.

4. Conclusion

Nanofibrillated cellulose was grafted in aqueous solution using a redox initiated free radical polymerization with two acrylates and three methacrylates. The method was both efficient and selective: graft copolymerization was dominant over homopolymerization with every monomer. The amounts of polymer grafted were generally higher than those reported in similar studies with macroscopic cellulose. The highest graft yields were achieved with BuA and GMA, both of which generated up to 80 wt% polymer in the product. However, their structures were very different. Molar mass measurements showed that PBuA formed very long chains, which were situated on the nanofibril surface fairly far apart. In the case of PGMA, XPS analysis suggested that there was a dense coating on nanofibrils and that polymer chains were relatively short. The other monomers formed smaller, yet significant, amounts of grafted polymer. Product composition was most effectively tuned by adjusting the amount of monomer. According to AFM imaging, the nano structure of the cellulose was preserved during synthesis, which means that the polymeric modification occurred without significant nanofibril aggregation. Structures of the grafted polymers varied from a thin coating to a continuous matrix completely enveloping the fibrils. This kind of modification may offer a simple way to improve the compatibility of NFC with synthetic polymers, removing one obstacle to strong cellulose-reinforced nanocomposites.

Acknowledgments

This work has been carried out as part of the project "Tailoring of nanocellulose structures for industrial applications (NASEVA)", funded by the Finnish Funding Agency for Technology and Innovation (TEKES). Forest Products Surface Chemistry research group of Aalto University is thanked for the AFM images and XPS, and VTT Technical Research Centre of Finland for solid-state NMR and TGA. Ritva Kivelä, Joseph Campbell, Sami Alakurtti, and Liisa Mansukoski are also acknowledged for the experimental work.

Appendix A. Supplementary data

Supplementary data associated with this article can be found, in the online version, at doi:10.1016/j.carbpol.2010.12.064.

References

Andresen, M., Johansson, L. S., Tanem, B. S., & Stenius, P. (2006). Properties and characterization of hydrophobized microfibrillated cellulose. *Cellulose*, *13*(6), 665–677.

Andrews, R. J., & Grulke, E. A. (1999). Glass transition temperatures of polymers. In J. Brandrup, E. H. Immergut, & E. A. Grulke (Eds.), *Polymer handbook* (4th ed., pp. 199–204). USA: John Wiley & Sons.

Beamson, G., & Briggs, D. (Eds.). (1992). *High resolution XPS of organic polymers: The scienta ESCA300 database.*. Chichester, England: Wiley & Sons.

Berglund, L. (2005). Cellulose-based nanocomposites. In A. K. Mohanty, M. Misra, & L. T. Drzal (Eds.), *Natural fibers, biopolymers and biocomposites* (pp. 807–832). Boca Raton: Taylor & Francis Group.

Bloch, D. R. (1999). Solvents and non solvents for polymers. In J. Brandrup, E. H. Immergut, & E. A. Grulke (Eds.), *Polymer handbook* (4th ed., pp. 501–502). USA: John Wiley & Sons.

Geacintov, N., Stannett, V., Abrahamson, E. W., & Hermans, J. J. (1959). Grafting onto cellulose and cellulose derivatives using ultraviolet irradiation. *Journal of Applied Polymer Science*, *3*(7), 54–60.

Gupta, K. C., Sahoo, S., & Khandekar, K. (2002). Graft copolymerization of ethyl acrylate onto cellulose using ceric ammonium nitrate as initiator in aqueous medium. *Biomacromolecules*, *3*(5), 1087–1094.

Habibi, Y., Goffin, A. L., Schiltz, N., Duquesne, E., Dubois, P., & Dufresne, A. (2008). Bionanocomposites based on poly (3-caprolactone)-grafted cellulose nanocrystals by ring-opening polymerization. *Journal of Material Chemistry*, *18*(41), 5002–5010.

Hase, T. (1999). *Tables for organic spectrometry* (8th ed.). Helsinki, Finland: Otatieto.

Jenkins, D. W., & Hudson, S. M. (2001). Review of vinyl graft copolymerization featuring recent advances toward controlled radical-based reactions and illustrated with chitin/chitosan trunk polymers. *Chemistry Reviews*, *101*(11), 3245–3274.

Marmur, A. (2008). From hygrophilic to superhygrophobic: Theoretical conditions for making high-contact-angle surfaces from low-contact-angle materials. *Langmuir*, *24*(14), 7573–7579.

Mishra, A., Srinivasan, R., & Gupta, R. (2003). P. psyllium-g-polyacrylonitrile: Synthesis and characterization. *Colloid & Polymer Science*, *281*(2), 187–189.

O'Connell, D. W., Birkinshaw, C., & O'Dwyer, T. F. (2005). A chelating cellulose adsorbent for the removal of cu (II) from aqueous solutions. *Journal of Applied Polymer Science*, *99*(6), 2888–2897.

Odian, G. (2004). *Principles of polymerization* (4th ed.). USA: John Wiley & Sons.

Okieimen, F. E. (2003). Preparation, characterization, and properties of cellulose-polyacrylamide graft copolymers. *Journal of Applied Polymer Science*, *89*(4), 913–923.

Okieimen, F. E, Uroghide, I. N., & Oriakhi, C. O. (1990). Graft copolymerization in aqueous isopropanol of methyl methacrylate on plantain pulp modified with allyl chloride. *European Polymer Journal*, *26*(2), 233–236.

Paakko, M., Ankerfors, M., Kosonen, H., Nykanen, A., Ahola, S., Osterberg, M., et al. (2007). Enzymatic hydrolysis combined with mechanical shearing and high-pressure homogenization for nanoscale cellulose fibrils and strong gels. *Biomacromolecules*, *8*(6), 1934–1941.

Roy, D., Semsarilar, M., Guthrie, J. T., & Perrier, S. (2009). Cellulose modification by polymer grafting: A review. *Chemical Society Reviews*, *38*(7), 2046–2064.

Shen, D., & Huang, Y. (2004). The synthesis of CDA-g-PMMA copolymers through atom transfer radical polymerization. *Polymer*, *45*(21), 7091–7097. doi:10.1016/j.polymer.2004.08.042

Stenstad, P., Andresen, M., Tanem, B. S., & Stenius, P. (2008). Chemical surface modifications of microfibrillated cellulose. *Cellulose*, *15*(1), 35–45.

Turbak, A. F., Snyder, F. W., & Sandberg, K. R. (1983). Nanofibrillated cellulose, a new cellulose product: Properties, uses, and commercial potential. *Journal of Applied Polymer Science: Applied Polymer Symposium*, *37*, 815–827.

Uschanov, P., Johansson, L., Maunu, S. L., & Laine, J. (2010). Heterogeneous modification of various celluloses with fatty acids. Cellulose, 1–12. doi:10.1007/s10570-010-9478-7.

Zahran, M. K. (2006). Grafting of methacrylic acid and other vinyl monomers onto cotton fabric using Ce (IV) ion–cellulose thiocarbonate redox system. *Journal of Polymer Research*, *13*(1), 65–71.

Zahran, M. K., & Mahmoud, R. I. (2003). Peroxydiphosphate-metal ion-cellulose thiocarbonate redox system-induced graft copolymerization of vinyl monomers onto cotton fabric. *Journal of Applied Polymer Science*, *87*(12), 1879–1889. doi:10.1002/app.11542